Thermodynamic properties of bulk and confined water

Francesco Mallamace,[1,2,3,a)] Carmelo Corsaro,[1] Domenico Mallamace,[4] Sebastiano Vasi,[5] Cirino Vasi,[5] and H. Eugene Stanley[3]
[1]*Dipartimento di Fisica e Scienza della Terra Università di Messina and CNISM, I-98168 Messina, Italy*
[2]*Department of Nuclear Science and Engineering, Massachusetts Institute of Technology, Cambridge, Massachusetts 02139, USA*
[3]*Center for Polymer Studies and Department of Physics, Boston University, Boston, Massachusetts 02215, USA*
[4]*Dipartimento di Scienze dell'Ambiente, della Sicurezza, del Territorio, degli Alimenti e della Salute, Università di Messina, I-98166 Messina, Italy*
[5]*IPCF-CNR, I-98166 Messina, Italy*

(Received 4 July 2014; accepted 26 August 2014; published online 15 September 2014)

The thermodynamic response functions of water display anomalous behaviors. We study these anomalous behaviors in bulk and confined water. We use nuclear magnetic resonance (NMR) to examine the configurational specific heat and the transport parameters in both the thermal stable and the metastable supercooled phases. The data we obtain suggest that there is a behavior common to both phases: that the dynamics of water exhibit two singular temperatures belonging to the supercooled and the stable phase, respectively. One is the dynamic fragile-to-strong crossover temperature ($T_L \simeq 225$ K). The second, $T^* \sim 315 \pm 5$ K, is a special locus of the isothermal compressibility $K_T(T, P)$ and the thermal expansion coefficient $\alpha_P(T, P)$ in the P–T plane. In the case of water confined inside a protein, we observe that these two temperatures mark, respectively, the onset of protein flexibility from its low temperature glass state (T_L) and the onset of the unfolding process (T^*).
 [http://dx.doi.org/10.1063/1.4895548]

I. INTRODUCTION

Expanding our understanding of water remains a topic of central interest in science and technology.[1] Water is ubiquitous throughout the universe and is fundamental in all biological processes. From the point of view of physical chemistry, it is a system that displays a complex thermodynamic behavior with many anomalies. The best known of these is its density maximum at 277 K. Other anomalous behaviors include such thermal response functions as its isothermal compressibility K_T, its isobaric heat capacity C_P, and its thermal expansion coefficient α_P. Structurally, it appears to be polymorphic in all of its phases: solid, glass, and liquid. Many studies of liquid water focus on its "diverging critical-like behavior" and understand it to be a function of its thermodynamic parameters. This is the same model as that proposed for supercooled glass-forming materials. The rationale behind the use of this model is straightforward: when the thermodynamic functions of liquid water are extrapolated from their values in the metastable supercooled phase (located between the homogeneous nucleation temperature $T_H = 231$ K and the melting temperature $T_M = 273$ K), they appear to diverge at a singular temperature ($T_S \simeq 228$ K at atmospheric pressure).[2] Below this temperature water is in its glassy form. Immediately above the glass transition temperature T_g, it becomes a highly viscous fluid and ultimately crystallizes at $T_X \approx 150$ K. The region between T_X and T_H is a "No-Man's Land" within which bulk liquid water cannot be studied experimentally.[2]

Unlike ice, which has many different crystalline structures that are determined by thermodynamic variables, amorphous water below $T_g \approx 130$ K has two phases. These are characterized by differing densities: low-density amorphous (LDA) and high-density amorphous (HDA) forms that can be switched back and forth by tuning the pressure.[3] Recently it has been suggested, theoretically and experimentally, that liquid water may also be a mixture of two liquids, low-density liquid (LDL), and high-density liquid (HDL), with an altered local structure that is a continuation of the LDA and HDA phases.[4–10] This theoretical and experimental work has elicited a number of hypotheses. Among them are the "liquid-liquid critical point (LLCP)" scenario,[4] the "singularity-free" scenario,[5] and the "stability limit" scenario,[6] all of which suggest that in the deeply supercooled single-component region of water there are two structurally distinct phases: a "low-density liquid (LDL)" and a "high density liquid (HDL)." Understanding these two phases is crucial if we are to understand the origin of the thermodynamic anomalies of water.

In addition to the above scenarios, it is commonly accepted that the hydrogen bond (HB) interactions among water molecules are key in understanding the anomalous behavior of water. Studies taking this approach assume the existence of (i) water "polymorphism"[11] and (ii) HB clustering, i.e., as T decreases, HBs begin to cluster and form an open tetrahedrally coordinated HB network.[1] These open local clusters have an ice-like density that is lower than the surrounding water.

Decreasing the T in the stable liquid phase causes the HB lifetime and cluster stability to increase. In principle, this altered local structure can continue through the No-Man's Land

a)Author to whom correspondence should be addressed. Electronic mail: francesco.mallamace@unime.it

down to the amorphous phase region. Hence in HDL, which predominates at high temperatures, the local tetrahedrally coordinated HB structure is not fully developed, but in LDL the HB network appears. The water anomalies appear to be the effect of these two local forms of liquid.

One model proposed for water, the so-called liquid-liquid critical point hypothesis, assumes water polymorphism and a first-order transition that indicates a special locus, the Widom line, in the T–P phase diagram at which the water thermodynamic response functions are at their maximum values.[12] This line of correlation length maxima can affect water response functions and can also explain their anomalous behavior.

Unfortunately this line and the associated polymorphic transition is difficult to study as it lies well inside the No-Man's Land, although many of the proposed theoretical scenarios assume that metastable liquid water exists below T_H.[4–8] Recently this hypothesis has been called into question by researchers using MD studies and finding that bulk water crystallization occurs more rapidly than the equilibration of LDL.[10,13] The only way to test the properties of liquid water in the deeply supercooled state is to retard crystallization by confining the liquid within nanoporous structures so narrow that it cannot freeze,[14] confining it within its own ice phase,[15] or by using electrolytic solutions.[16,17]

In one sense we might consider confined water to be more essential than bulk water, i.e., the behavior of confined liquid water strongly impacts the biological functionality of all living species and the chemical-physical properties of natural and synthetic materials. Water is essential in the functioning of micro- and nano-structured systems, e.g., proteins, membranes, and the living processes of cells. Water is key in maintaining the structure, stability, dynamic behavior, and functionality of biological macromolecules. Examples include the reversible protein folding-unfolding process in which water mediates the collapse of the chain and the search for the native topology through a funneled energy landscape[18] and the protein "dynamic" transition that biomolecules undergo in the low-T regime.[19] At the lowest temperatures proteins exist in a glassy state, a solid-like structure without conformational flexibility.[20] There are thus many reasons why liquid water should not be treated as a solvent only, but rather as an integral and active component of biomolecular systems, i.e., it is itself a "biomolecule" with fundamental dynamic and structural roles.[21] These bio-systems also suggest that hydrogen bond (HB) interactions between water molecules (and within biomaterials) are key to understanding their properties and functioning.[22]

Many experiments have been done on confined water in nanopores[14,23,24] and biological macromolecules[25–39] in the stable liquid phase and in the supercooled regime. Different experimental techniques have been used, e.g., light and neutron scattering, dielectric relaxation, nuclear magnetic resonance (NMR), Mössbauer, optical Kerr-effect, and electron spin resonance (ESR) spectroscopy.[40] Some of these studies clearly show, at ambient pressure, that when T is decreased to a certain point the water HB lifetime increases by approximately six orders of magnitude, indicating the Widom line is crossed at $T_L \simeq 225$ K where a fragile-to-strong dynamic crossover occurs,[12,14] the Stokes-Einstein relation is violated,[23,41] and LDL local structure predominates over HDL.[14,24] Note that a fragile-to-strong dynamic crossover was initially predicted for bulk water at $T_L \simeq 225$ K.[42] Previous results have also been confirmed for such "open confinements" of water as water in methanol,[43] water in ice,[15] and water in a solution of eutectic LiCl.[17] In the latter two cases water is localized in nano-pools containing enough molecules that the water can be treated as though it were in bulk form. Thus "open confinements" and aqueous LiCl solution scenarios have been considered suitable models for bulk water.

Note that all the problems regarding the chemistry and physics of both bulk and confined water are strongly debated, in many cases with diverse interpretations of MD simulation studies and of experimental results. In MD simulations, the results are dependent on the model and the water potential used,[9] and in experiments the results depend on instrumental sensitivity. One example is the fragile-to-strong dynamic crossover that is accompanied by the violation of the Stokes-Einstein (SE) relation with a fractional behavior, where a decoupling between the translational and the rotational diffusion (for $T < T_L$) takes place.[44] In the high T-regime, as evidenced by the SE, the translational diffusion, D_s, tracks the inverse of the shear viscosity (η^{-1}). Whereas for $T < T_L$, D_s declines far less rapidly by decreasing T as $D_s \sim \eta^{-\xi}$, with $\xi \simeq 0.75$, D_{Rot} (the rotational correlation time) remains proportional to the inverse of the shear viscosity down to T_g. For this reason any experimental technique that only takes rotational motion into account may be not fully sensitive to the dynamic crossover.

The dynamic crossover temperature T_L, like the glass transition temperature T_g, is relevant and important when examining many materials in the liquid supercooled phase[45,46] and hence is also important when studying water. It can be used as a reference point for hydrated systems when examining how solvency influences the properties of complex supramolecular systems with a mesoscopic structure. It has been suggested, for example, that the agreement in crossover temperature with the temperature predicted for neat water means that the crossover in water drives protein dynamics. However, protein hydration water, like water in mesosystems (polymers, gels, polyelectrolytes, cells), is in a heterogeneous environment made of hydrophobic, hydrophilic, and charged groups in which the behavior of water is expected to be strongly modified. This question continues to be strongly debated.

Complex materials such as water are characterized by rich phase diagrams. To study them we must focus on all the variables, i.e., pressure, concentration, and interactions all strongly influence their thermodynamic properties. An analysis of the P–T behavior of water density reveals that the maximum dominating the thermodynamics of the system under ambient conditions, is strongly P-dependent, and disappears at a crossover pressure $P_{\mathrm{cross}} \sim 1.8$ kbar. In addition, the isothermal compressibility $K_T(T, P)$ shows a minimum at $T^* \sim 315 \pm 5$ K for all the pressures in the range $1 < P < 9 \times 10^3$ bar, whereas the coefficient of thermal expansion $\alpha_P(T, P)$ has a surprising behavior: all the $\alpha_P(T)$ curves measured at different P cross at T^*.[47] The experimental data[6,48–55] show a "singular and universal expansivity point" at $T^* \sim 315$ K

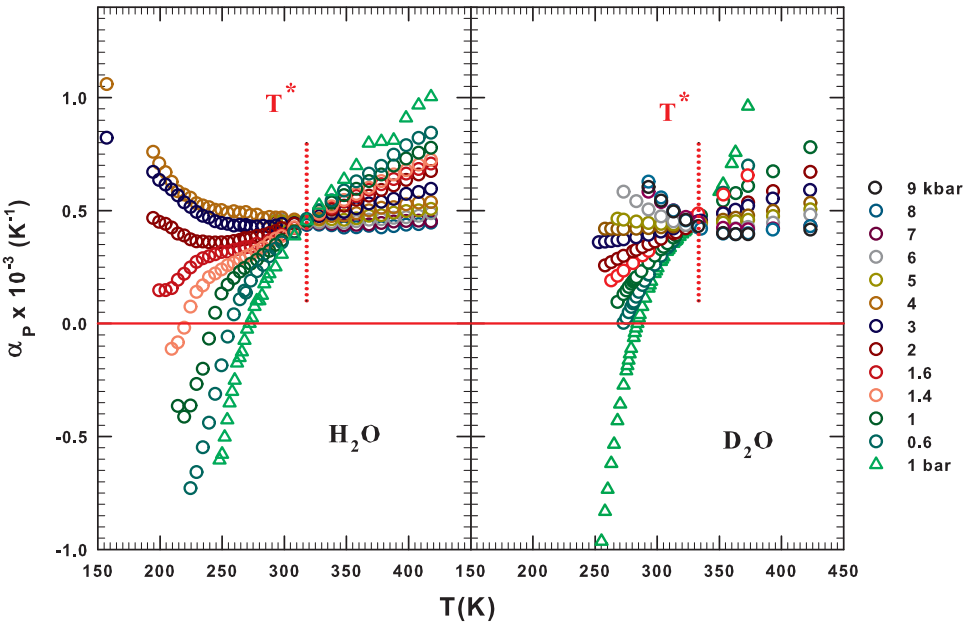

FIG. 1. The coefficient of thermal expansion for bulk (left panel) and heavy (right panel) water as a function of the temperature at different pressures. In both panels, the temperature (T^*) that marks the border between simple and complex behavior is highlighted (dotted line). This temperature does not depend on pressure as data at different pressure cross each other there.

and $\alpha_P(T^*) \simeq 0.44\ 10^{-3}\ \mathrm{K}^{-1}$. Figure 1 reports such a situation for both H_2O and D_2O, where the dotted line identifies T^*. Unlike other water singularities, this temperature is thermodynamically consistent in the relationship connecting the two response functions $(\partial\alpha_P/\partial P)_T = -(\partial K_T/\partial T)_P$. Whereas K_T ($K_T = (\partial \ln\rho/\partial \ln P)_T = -V^{-1}(\partial V/\partial P)_T$) is related to volume fluctuations δV as $K_T = \langle\delta V^2\rangle_{P,T}/k_BTV$, $\alpha_P(T,\ P)$ ($\alpha_P = -(\partial \ln\rho/\partial T)_P = -V^{-1}(\partial S/\partial P)_T$) represents the entropy and volume cross-correlations $\langle\delta S\delta V\rangle$ being $\alpha_P = \langle\delta S\delta V\rangle/k_BTV$.

We thus note that T^* represents a basic property of liquid bulk water. Furthermore, when we consider a thermodynamic transport parameter such as the bulk water self-diffusion coefficient $D_S(T,\ P)$, measured for different pressures ($1 < P < 10^4$ bar) in the range $252 < T < 400$ K, we see that $T^* \sim 315$ K marks the crossover between two different physical realities: below T^*, $D_S(P)$ has a maximum that for $T = 252$ K is located at ≈1600 bar, and that, as T increases, $D_S(P)$ evolves at the lowest P and disappears near T^*. When $T > T^*$, the $D_S(P)$ behavior becomes regular. An Arrhenius plot, ($\ln D_S$ vs. $1/T$), of D_S at constant P also reveals that T^* marks two different regions:[47] when $T > T^*$ the thermal behavior of the self-diffusion coefficient is simply Arrhenius ($D_S = A\exp(E/k_BT)$), but in the range from T^* to the supercooled regime the self-diffusion behavior is super-Arrhenius. The Arrhenius activation energy ($T > T^*$) obtained from the data fitting is $E = 15.2 \pm 0.5$ kJ/mol, i.e., the HB energy value, which fully supports the primary role of HBs in the properties of water.

Hence T^* marks a transition from an high-T region characterized by a water molecular dynamic with only one energy scale (the Arrhenius energy) to another dynamic typical of supercooled glass-forming liquid systems in which the intermolecular interactions (correlations in the time and length scale, i.e., dynamic clustering) increase as T decreases, causing the formation of the HB tetrahedral network. Glass-forming liquids in the supercooled regime, like complex materials, are dominated by the interaction processes originating in the disordered and finite correlation regions (finite polydisperse dynamic clustering) that the transport parameters (relaxation times, viscosity, and self-diffusion) reflect by means of a super-Arrhenius behavior or a multi-relaxation in the time evolution of the density-density correlation functions. Liquid state theory suggests the existence of a temperature marking a crossover from normal liquid behavior to supercooled behavior.[5,56–58] Above that temperature the transport is Arrhenius and below it the correlations cause activation barriers to increase with a growing scale resulting in a super-Arrhenius behavior, i.e., a change in the explored configuration space.[5,56,58,59] This behavior dominates the liquid approaching dynamic arrest by means of local potential minima in its energy landscape.[5,60,61] A liquid under normal conditions experiences local dynamics in the interaction basins surrounding the minima and rearranges itself via intrabasin motions and relatively infrequent interbasin jumps. As the temperature decreases and approaches the glass transition, as in the clustering process that dominates complex material dynamics, jump dynamics become more dominant than intrabasin dynamics and, in addition, the molecular interactions impose a leveling of the energy barriers. At this point, the dynamic behavior switches from super-Arrhenius to pure-Arrhenius, giving rise to the dynamic crossover that characterizes glass-forming liquids.[62]

This scenario of the physical meaning of T^* was confirmed by using the Adam-Gibbs approach to consider D_S ($1/D_S \sim \exp(C/TS_C)$) and relating this transport coefficient to the configurational entropy, S_C, and the NMR proton chemical shift δ (where both are an approximate measure of the

local order sampled by the liquid water molecules in the configurational space).[59] Using S_C and δ, we see that at T^* the water local order indicates, as T decreases, the crossover from a normal liquid to an anomalous and complex liquid.[63]

Being experimentally certain that T^* plays a fundamental role in bulk liquid water thermodynamics and that T_L is the temperature of primary interest when examining the arrest of water dynamics, we next explore whether these two temperatures can characterize confined water.[47,63] This allows us to clarify similarities and differences between the properties of these two types of water. In many supercooled liquids, e.g., OTP (ortho-terphenyl),[61] T_L has been observed experimentally in the bulk liquid phase on approaching the arrest temperature.[45,46,62,64–66] T_L is localized above T_g (usually $T_L \simeq 1.2T_g$) and represents the locus of the fragile-to-strong dynamic crossover (FSDC), the violation of the Stokes-Einstein, and the temperature at which the dynamic heterogeneities have their onset. Recently, T_L has been recognized as important in understanding how systems approach DA, since a lot of exceptional processes disclose their properties at that temperature.[45,64] Many studies predict that $T_L \approx 225$ K in liquid water.[12,41,42,67,68] In particular, using the Adam-Gibbs approach[59] it has been proposed that the fragile-to-strong transition in supercooled water occurs near 228 K "corresponding to a change in the liquid's structure at this point"[42] and to the dominance of LDL local structure over HDL.[14,24,41] In contrast, other studies[46,64,65,69] propose a power law behavior in transport parameters, e.g., $D_S \sim |T - T_L|^{-\gamma}$, and obtain approximately the same crossover temperature. Unfortunately, T_L cannot be observed in bulk water, although there are significant experimental signs of its existence. For example, the sound propagation and the marked viscoelastic behavior observed (a dependence on the experimental power spectrum $S(Q, \omega)$ on the wavevector Q and the frequency ω) is fully consistent with the possibility that bulk water behaves like confined water, which would indicate that $T_L \approx 225 \pm 5$ K, assuming it could be supercooled to that temperature range.[70]

II. EXPERIMENTS

We consider experimental data of bulk and confined water on the surface of a protein (hydration or external water) and in nanotubes. These data are obtained using nuclear magnetic resonance (NMR) spectroscopy. In particular, we measure the self-diffusion (D_s), the proton spin-lattice (T_1) relaxation time, and the proton local order (proton chemical shift δ) to evaluate the configurational specific heat.[71] We use globular protein lysozyme hydrated with a single monolayer of water and silica nanotubes MCM-41. The protein sample is prepared according to a precise procedure.[31] The dried protein powder is hydrated isopiestically at 5°C by exposing it to water vapor in a closed chamber until the wanted hydration level $h = 0.3$ and $h = 0.32$ is obtained (i.e., grams of H_2O per grams of dry protein). In both systems, differential scanning calorimetry was used to test the absence of bulk-like water. The micelle-templated mesoporous silica matrix MCM-41-S, synthesized using the zeolite seeds method, are 1D cylindrical tubes arranged in a hexagonal structure. The pore size was determined using a nitrogen absorption-desorption technique.[14] We used fully hydrated MCM-41-S samples with $d = 14$, 18, and 24 Å at ambient pressure. We study the dynamic water properties at ambient pressure and in the temperature range 200 K–370 K (with an accuracy of ±0.2 K) using a Bruker AVANCE NMR spectrometer operating at 700 MHz (^{1}H resonance frequency). The T-dependence of the chemical shift of methanol was used as a T standard. We study samples using cooling or heating cycles that produce the same spectra. We begin at 296 K and cool the samples in 5 K steps down to 200 K and then reverse the procedure, but keep the samples for several hours at $T = 200$ K before heating. We measure the self-diffusion coefficient D_s using the pulsed gradient spin-echo technique (^1H-PGSE[72]) and measure T_1 using the standard inversion recovery pulse sequence ($[\pi - t - \pi/2$ − acquisition], where t denotes the time between the two RF pulses. We measure the chemical shift δ using free-induction decay (FID).

Note that the NMR technique directly probes the local order around a single atom of a given material. Specifically, it measures the proton chemical shift δ that represents the effect of the interaction of water with its surroundings, and that it provides, in particular, a rigorous picture of the intermolecular geometry.[73] Hence δ represents the average number of HBs with which a water molecule is involved at a certain point in the P–T phase diagram, $\langle N_{\rm HB}\rangle$. Note that δ is a linear response of the electronic structure of the system to an external magnetic field B_0 as $B(j) = (1 - \delta_j)B_0$, where j is an index that identifies the chemical environment.[74,75] In particular, δ is related to the magnetic shielding tensor σ which in turn is related to the local field experienced by the magnetic moment of the observed nucleus and is strongly dependent on the local electronic environment. Hence the chemical shift is a useful probe of the local geometry and in particular of the hydrogen bond structure for water and aqueous systems and solutions.[76] Water in both the normal liquid and supercritical liquid regions exhibits a direct relationship between $\delta(T)$ and the average number of HBs, $\langle N_{\rm HB}\rangle$, with which a water molecule is involved, i.e., $\delta(T) \propto \langle N_{\rm HB}\rangle$.[73,77] This is the precise experimental procedure by which we obtain δ.[71,73]

Because $\langle N_{\rm HB}\rangle$ is related to the number of possible configurations of the water molecules in the HB network, the system configurational entropy can be written as $S_c \approx -k_B \ln \langle N_{\rm HB}\rangle$. Hence using NMR data we can evaluate the configurational specific heat $C_P^c(T)$ ($C_P = T(\partial S/\partial T)_P$) as

$$C_P^c(T) \approx T\left(\frac{\partial S_c}{\partial T}\right)_P \approx -T\left(\frac{\partial \ln\langle N_{\rm HB}\rangle}{\partial T}\right)_P \approx -T\left(\frac{\partial \ln \delta(T)}{\partial T}\right)_P. \quad (1)$$

III. RESULTS AND DISCUSSION

Using the proton local order to evaluate the configurational specific heat, as described above, we examine the obtained $C_P^c(T)$ data for confined water.

Figure 2(a) shows $C_P^c(T)$ obtained for water confined in MCM nanotubes. It also shows the corresponding data, obtained using the customary calorimetry, for bulk water (in

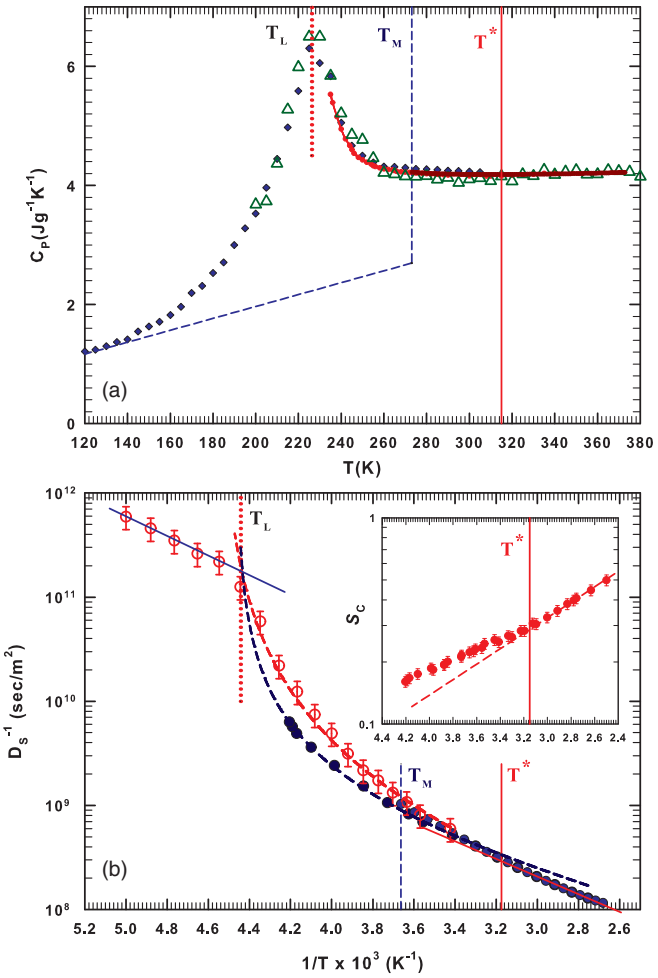

FIG. 2. (a) The isobaric specific heat for bulk and confined water as a function of the temperature. In the panel, the temperatures of the minimum (T^*) and maximum values (T_L) are reported together with the values for ice and the melting point (T_M). Blue diamonds refer to calorimetric measurements on water confined in MCM, green triangles refer to specific heat data obtained by NMR (C_P^c), and red circles refer to bulk water. (b) The inverse of the self-diffusion coefficient for bulk (filled dark blue circles) and confined water (open red circles) obtained by the NMR technique as a function of the temperature. The configurational entropy, obtained through the Adam-Gibbs relation, is reported in the inset. It is noteworthy that the thermal behavior of D_S^{-1} evidences important variations at the highlighted temperatures T^* and T_L. The red and blue dashed lines represent the data fitting with a power law for confined and bulk water, respectively. The straight line in the strong Arrhenius regime is the best fit of the data with an activation energy of 16.7 kJ/mol.

the interval $245 < T < 373$ K)[9,78] and for water confined in the same silica nanotubes (MCM-41, $d = 12$ A, $120 < T < 300$ K).[79] The $C_P^c(T)$ data obtained from $\delta(T)$ are adapted to the true calorimetric data in terms of a multiplicative factor. Note that all these data display an analogous thermal behavior and, within the error bars, there is good agreement between the different C_P data. For comparison, the specific heat ice data are also reported (dashed line). By considering the two characteristic temperatures discussed above, T_L and T^*, we observe that they coincide with the temperatures of the $C_P^c(T)$ maximum and $C_P(T)$ minimum, respectively. Regarding T^*, we stress that whereas $-T(\partial \ln \rho/\partial T)_P$ is directly related to the cross-correlation between the entropy and volume fluctuations $\langle \delta S \delta V \rangle$, C_P is proportional to the square of the entropy fluctuations $\langle \delta S^2 \rangle$.

Figure 2(b) shows the Arrhenius plot of the inverse of the measured self-diffusion coefficient (D_s^{-1}) of nanotube-confined water (open red circles) and compares it with bulk water measured in the supercooled phase (filled dark blue circles)[80] and in the stable liquid phase (filled blue circles).[81] Note that although when $T > T_M$, the D_s^{-1} data of bulk and confined water are nearly coincident, when $T < T_M$ the situation is very different, especially when T decreases toward T_L. In both bulk and confined water cases, the data can be fitted with the above proposed power law form ($D_s^{-1} \sim |T - T_L|^{-\gamma}$), obtaining $T_L \simeq 223$ K and $\gamma \simeq 1.96$ for bulk water and $T_L \simeq 225$ K and $\gamma \simeq 2.19$ for water confined in nanotubes. Only in the confined water case, however, it is possible to effectively observe how the dynamic crossover temperature affects water properties. The T^* crossover is intriguing in that it allows us to explore the water properties that emerge from bulk water in the stable liquid phase. From the D_s^{-1} data in the high temperature regime, T^* represents a new dynamic crossover. Specifically, the water dynamics change when decreasing T causes a shift from Arrhenius to super Arrhenius behavior. Using the Adam-Gibbs approach[59] and connecting the configurational entropy and the transport parameters, we calculate S_C at each T from the bulk water D_s^{-1} data (filled dark blue circles). The results are reported in the inset of Fig. 2(b). This clarifies the effect of T^*, i.e., it represents the temperature at which the behavior of the local order of the system changes.

Figure 3 shows the temperature behavior of the spin-lattice relaxation time T_1, which provides further information on the dynamics of confined water. It displays many data, in particular: bulk water data including data supplied by Ref. 81 (filled dark blue circles), data we collected (dark blue empty circles), data from MCM-41 nanotubes of diameter 14A (red circles), data from MCM-41 nanotubes of diameter 24A (dotted circles), data from a water-methanol solution at methanol molar fraction $X = 0.04$ (dark blue triangles), and data from a water-methanol solution at methanol molar fraction at $X = 0.1$ (blue triangles). Figure 3 also shows data from a NMR experiment in water at high pressure (2.25 kbar) at frequencies 255 MHz (dark red squares) and 362 MHz.[82] On looking at the figure it can be noticed that all these relaxation time data can, within the error bars, be superimposed. A care analysis of the T-behavior of these data can confirm, also taking into account previous studies on transport properties of bulk water,[81,83] the role and the importance, in water dynamics, of T_L and T^*(reported in Figure 3 as dotted and straight lines, respectively). Although the data in the T_1 case are at high pressure, the suggestion of a fragile-to-strong dynamic crossover occurring at T_L seems to be confirmed. Figure 3 also shows, in the high T-regime, data on bulk water viscosity $\eta(T)$[83] reported as $T\eta^{-1}$ (small filled red circles). Note that these data do not agree with the spin lattice T_1 data. Simpson and Carr[81] "in the first direct measurement of the proton diffusion in water as a function of temperature" in 1958 considered $D_s(T)$, $\eta(T)$, and the spin lattice relaxation time and found that although the Stokes-Einstein relationship adequately describes bulk water, T_1 is decoupled from the viscosity just at about

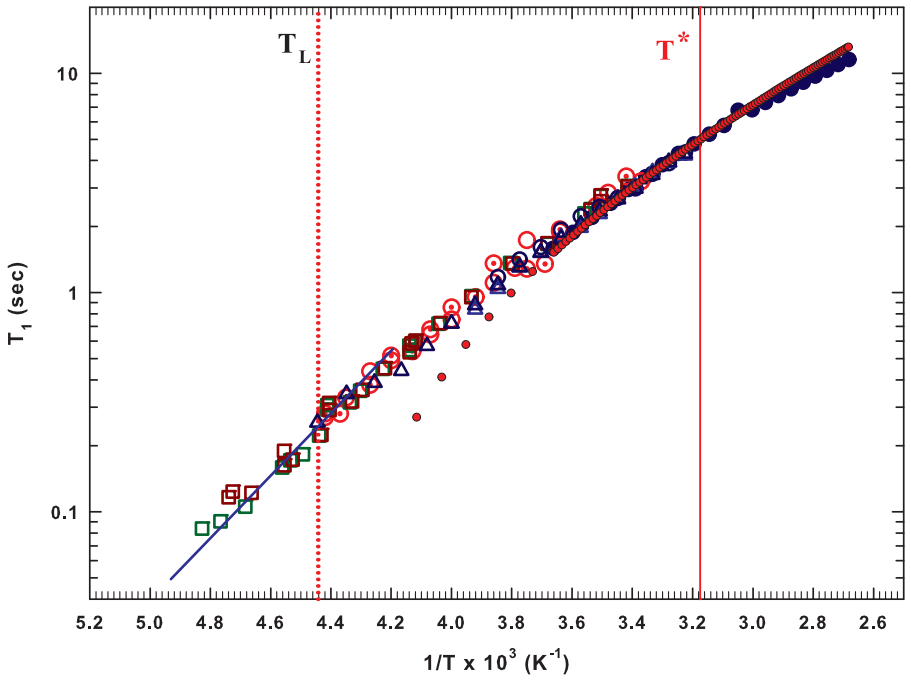

FIG. 3. The proton spin-lattice relaxation time for bulk (filled blue circles), confined water and water in solution as a function of the temperature. Open circles refer to water confined in MCM, open squares refer to water at high pressure (2.25 kbar), and open triangles refer to water/methanol solution with methanol molar fraction $X = 0.04$ (light blue triangles) and $X = 0.1$ (dark blue triangles). Spin-lattice (T_1) relaxation data superimpose each other and seem to show a fragile to strong crossover at T_L. The straight line is a guide for eyes. Small red circles represent $T\eta^{-1}$ and allow appreciating the deviation of this quantity from T_1 just at T^*, as previously demonstrated.[81]

T^*. In fact, when T is increased a "major" deviation appears at ≈315 K (see Fig. 2(a)), the location of the isobaric specific heat minimum.

When we examine the system water-protein lysozyme, including both internal and hydration water,[21] we find two temperatures of central importance. In one there is an onset of biological activity, in the other the biomaterial irreversibly denatures. As mentioned above, these temperatures correspond to the low-T protein "dynamic" transition[19] and the protein folding-unfolding process, respectively.[18]

At the lowest temperatures proteins exist in a glassy state, a solid-like structure without conformational flexibility.[20] By increasing T, the protein atomic motional amplitude, measured by looking to the proton mean-squared displacement $\langle X^2 \rangle$ (MSD), increases linearly, as in a harmonic solid. In hydrated proteins $\langle X^2 \rangle$ suddenly increases at ∼220 K, signalling the onset of a liquid-like motion (nonharmonic and less rigid).[19,26] The functions and the kinetics of biochemical reactions of many proteins slow sharply at a temperature, T_C, in a universal interval 240–200 K.[25,84] This transition appears to be solvent dependent and is suppressed in dry biomolecules.[26] The bioactivity of the proteins is dependent upon their level of hydration, h. For lysozyme, the hydration level $h = 0.3$ corresponds to a water monolayer covering the protein surface, and its enzymatic activity is very low up to a hydration level of 0.2. It then increases sharply for $0.2 < h < 0.5$.[85]

Water can influence both the biomolecular hydrophilic and hydrophobic side groups. The hydrophilicity is a force that governs the secondary structure and folding specificity in proteins,[86] but the properties of the biomolecule can also be affected by the protein methyl groups, which are a factor in the dynamic transition. Because the properties of the surface water (the first layer water network) are intimately connected to protein stability and function, hydrophilic interactions with peptide groups are the most important topic when studying biological systems. The approximate coincidence of T_L (the water dynamic crossover) and T_C (the onset of the protein biochemical activities) accompanied by the sharp rise in $\langle X^2 \rangle$, has suggested that this "dynamic" transition in proteins can be triggered by their strong hydrogen bond coupling with the hydration water.[87] This behavior has been observed in several biomolecules including globular proteins.[88] This protein crossover has been studied by measuring the MSD (neutron experiments) and the transport parameters (NMR) and it has been related to the protein "softness" resulting from its conformational disorder.[26]

A protein remains in the native state up to a given temperature and evolves, on increasing T, into a region characterized by a reversible unfolding-folding process. This latter phenomenon is dependent upon the chemical nature of the protein and the solvent. For water-lysozyme it occurs in the range 310 K $< T <$ 360 K. The protein unfolding is characterized by a well defined broad peak in C_P with a maximum at $T_D \simeq 346$ K.[89] For $T \geq T_D$, lysozyme denatures irreversibly. The process rate constant varies as a function of T in accordance with an Arrhenius law. It has an activation energy that is typical of the HB strength and thus confirms the primary role of water in this transition. The dramatic change in the protein structure is driven by the HBs between the protein and its hydration water.[35] This latter quantity is strongly related to the chemical shift $\delta(T)$.

Figure 4(a) shows the configurational specific heat data of the hydrated protein for $h = 0.3$ and $h = 0.32$ (as proposed for water in MCM, Fig. 2(a)). Figure 4(b) shows the same for D_s^{-1} across a very large T −range ($200 < T < 370$ K), which includes all the significant protein phases: the glass, the native, and the reversible and irreversible unfolding-folding processes. Figure 4 also shows the temperature T_D of the C_P maximum together with T_L and T^*. In Figure 4(a), the configurational C_P^c obtained from $\delta(T)$ data and the "direct" C_P[89] are shown as a T-function. Figure 4(b) shows the NMR D_s^{-1} data in an Arrhenius plot as a function of the reduced temperature $1000/T$. Figure 4(a) uses a double scale plot to show $(-T\partial \ln \delta(T)/\partial T)_P$ for lysozyme hydration water (on the left) and the C_P measured in the temperature region including the reversible unfolding-folding process (on the right). Note that $(-T\partial \ln \delta(T)/\partial T)$ displays two maxima, the first on crossing T_L, as proposed by experiments and simulation studies on hydrated proteins,[31,90] and the second nearly coincident with T_D, associated with the protein denaturation process. The first maximum at ≈230 K is at the same temperature, within the error bars, as the confined water dynamic crossover. This confirms that both are due to the same

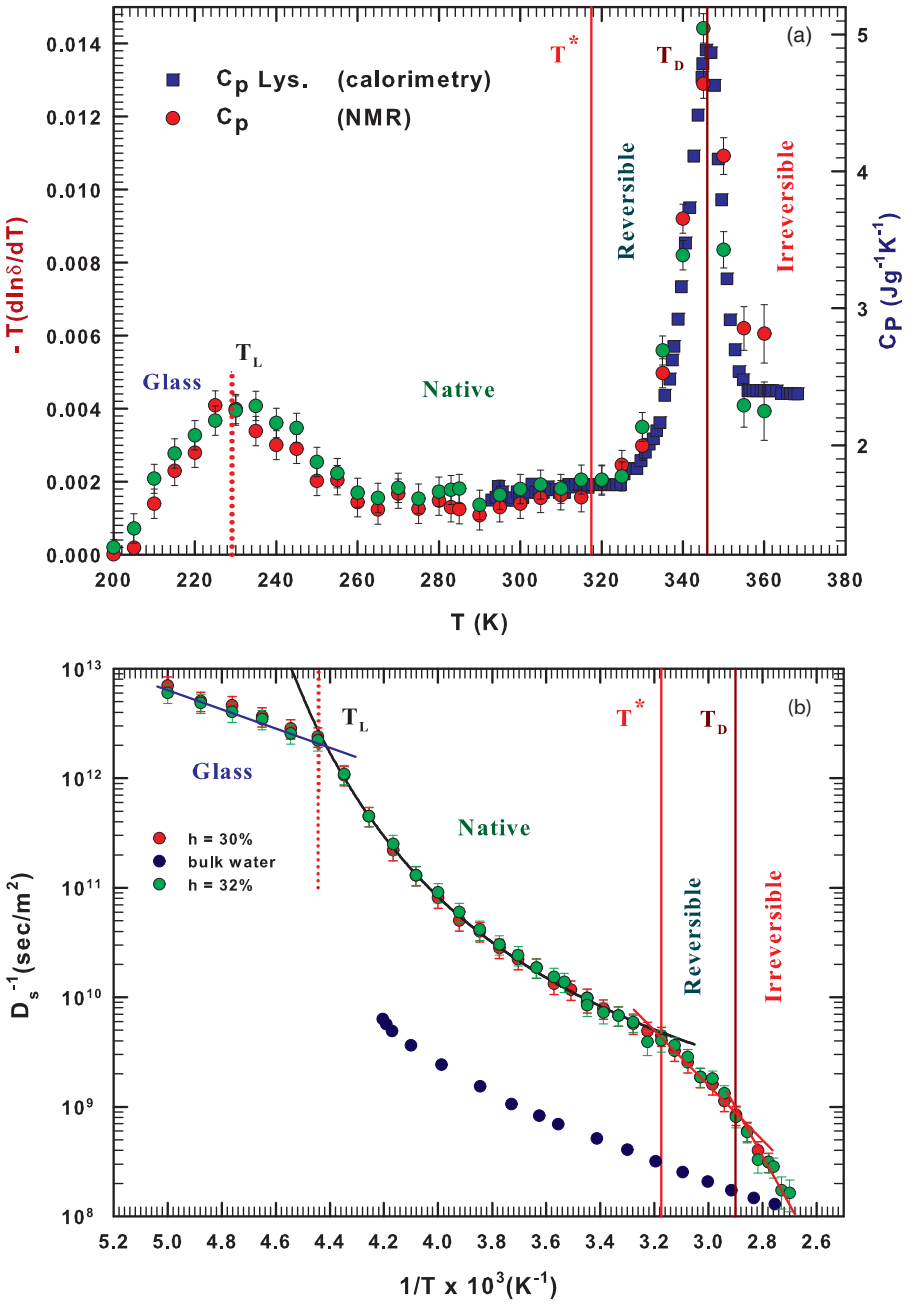

FIG. 4. (a) The isobaric specific heat for lysozyme hydration water, obtained by modulated scanning calorimetry (blue squares), and its configurational counterpart obtained by means of NMR, as a function of the temperature. The temperatures at which this quantity displays two maxima are just T_L and T_D that, together with T^*, define the interval of lysozyme biological activity. (b) The inverse of the self-diffusion coefficient for bulk (filled dark blue circles) and lysozyme hydration water (filled red and green circles) obtained by the NMR technique as a function of the temperature. Also in this case, the thermal behavior of D_S^{-1} evidences important variations at the highlighted temperatures T^*, T_L, and T_D. The straight lines are guides for eyes.

structural change in water, and that the LDL phase dominates the properties of water at T_L.[12,14,17,23,24,41,67,68]

Prefactors aside, the $\delta(T)$ derivative and the C_P data support the physical idea that the observed behaviors originate in changes in the configurational entropy. Because $\delta(T)$ is related to the *orientational* local order and not the *translational* local order, we find that the contribution of the orientational disorder to entropy is dominant. This confirms the protein structural picture in the low temperature regime where the neutron scattering data on $\langle X^2 \rangle$ (MSD) indicate that there is a change in the protein "softness" and that our C_P^c data relate directly to the protein structural changes. This approach is confirmed by how the protein behaves when the temperature is increased toward the maximum and the protein unfolds or denatures (or the reverse during the folding process). In the first case, the protein behaves like a polyelectrolyte in a bad solvent that imposes an abrupt change in the structure, from compact, to swollen, and to an open structure dominated by large fluctuations.[91] Here the HB strength between water and the hydrophilic protein groups are dominated by the hydrophobic interaction for which water molecules prefer a more direct interaction rather than with the polyelectrolyte. This happens in a temperature regime around T^* where the HB lifetime is reduced to a fraction of picoseconds. In contrast, around T_L the HB lifetime is measured in microseconds and is five orders of magnitude larger. This behavior is reflected in the D_s^{-1} data shown in Fig. 4(b). When the temperature of water is decreased its solvency increases and, through its HB interactions, it is able to be the active component of biomolecular systems, determining their dynamic and structural properties.[21] It is well known that HBs govern the secondary structure in proteins and the specificity of folding.[86] At the same time, the role the HBs in water plays in protein folding, in protein-protein binding, and in molecular recognition constitutes the basis for the hydrated protein thermodynamic behavior, as heat capacity effects.[92] In short, water acts as a HB "glue" between the carbonylic and amidic groups of a protein.[93] All these statements confirm the validity and the reported data of the configurational specific C_P^c obtained from the proton local order in the water lysozyme system.

Note that all the observed behaviors are the effects of hydration and protein internal water. Figure 4(b) confirms this with an Arrhenius plot of $D_s^{-1}(T)$. Note also that the measured activation energies agree with the HB energies. We see the dynamic crossover at T_L in water confined around the protein that appears to be universal, at least for confined water (we cannot verify this in bulk water). Figure 4(b) also shows the self-diffusion data corresponding to bulk water (filled blue circles). Note that the thermal behavior of bulk and protein confined water is similar in the native phase, although there is a difference of approximately one order of magnitude in their corresponding values (the dynamic behavior of bulk water is faster than that of hydration water). We note that the T^* temperature indicates two changes in both C_P^c and D_s^{-1}. For the self-diffusion coefficient T^* indicates that when T is increased there is a dynamic crossover; for the configurational specific heat it represents instead the locus at which C_P^c begins to increase toward the maximum. This is an important indicator of the onset of the unfolding process. A previous experiment has

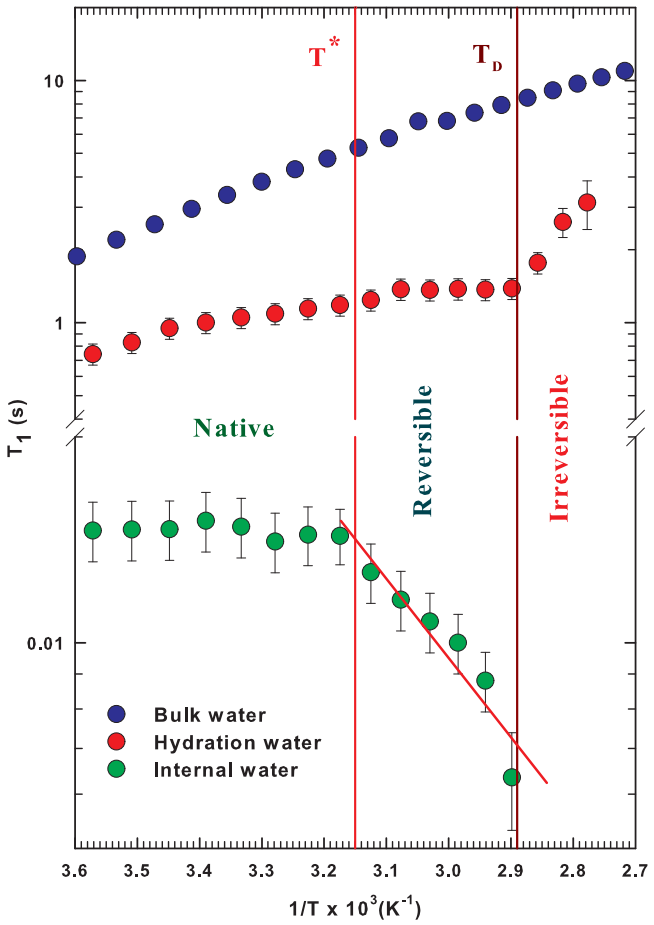

FIG. 5. The proton spin-lattice relaxation time for bulk (blue circles) and lysozyme water (internal, green circles, and hydration, red circles) in the thermal region of the folding/unfolding process. It is noteworthy that both these two last contributions show the first change at T^* and that just above T_D the lysozyme internal water contribution becomes negligible (inversion recovery data are fitted by a single exponential function) and the T_1 values of hydration water evolve toward those of bulk water on increasing temperature. This means that lysozyme residuals are essentially open and the internal (or crystallization) water becomes free as well as hydration water and resemble the bulk behavior. The straight line is a guide for eyes.

demonstrated this by performing heating and cooling cycles in the same system and finding that the reversibility stops at T_D.[35] We see another change for $T > T_D$ in which $D_s^{-1}(T)$ evolves quickly toward the bulk water value. Figure 5 clarifies this by showing the behavior of the corresponding proton spin-lattice relaxation time T_1, providing data on bulk water (filled dark blue circles), T^*, and T_D, which are characteristic of the unfolding/folding process. As mentioned above in Sec. II, the spin-lattice relaxation time is obtained by using a pulse sequence that gives the proton magnetization time-dependent spectrum $M(t)$.[76] In simple liquids, $M(t)$ is usually characterized by a single exponential decay. In an actual case, protein water magnetization is characterized by two time contributions: one that is slow due to hydration water (T_1^{slow}) and one that is fast due to the internal protein water (T_1^{fast}).[31,94] Figure 5 shows both the slow contribution (filled red circles) and the fast contribution (filled green circles). In the native phase these two spin-lattice relaxations change slowly with T (with T_1^{fast} nearly constant), but above T^* there is a rapid

decrease in T_1^{fast} that terminates at approximately T_D above which only one contribution (T_1^{slow}) can be detected in $M(t)$. For the region of the unfolding irreversibility $T > T_D$, this remaining contribution is characterized by a marked slowing down toward the bulk water T_1 value, a behavior analogous to that observed in D_s^{-1}. It is evident from these data that above the irreversible denaturation threshold there is no distinction between internal and hydration water: all water molecules can diffuse freely.

IV. CONCLUSIONS

Bulk water is characterized by two singular temperatures in the high temperature regime of the thermal stable liquid phase and in the low metastable supercooled region.

The first temperature, $T^* \sim 315 \pm 5$ K, characterizes two basic thermodynamic response functions: (i) the isothermal compressibility $K_T(T, P)$ and (ii) the thermal expansion $\alpha_P(T, P)$. T^*, where the isothermal compressibility $K_T(T, P)$ shows a minimum for all the measured pressures (in the range $1 < P < 9 \times 10^3$ bar), is also a *special locus* of the thermal expansion $\alpha_P(T, P)$. All the $\alpha_P(T, P)$ curves measured at different P cross each other at T^*,[47] indicating a universal expansivity point. For H_2O, the coordinates of this point in the $T - \alpha$ plane are T^* and $\alpha_P(T^*) \simeq 0.44 \times 10^{-3}$ K^{-1}. In particular, both $K_T(T, P)$ and $\alpha_P(T, P)$ display the anomalies that characterize the system in the supercooled metastable regime.

The second temperature, T_L, is at the fragile-to-strong dynamic crossover, which much recent literature suggests is a general phenomenon characterizing properties of supercooled glass-forming liquids at dynamic arrest.[45,46,62,64–66] Using theoretical considerations and MD computer simulations,[12,41,42] this crossover has been hypothesized to be ≈225 K for bulk water (it is experimentally observable only in confined water). Using NMR spectroscopy and taking these considerations into account, we have studied the dynamics of water confined in different environments and in its bulk phase across a large temperature range, one that covers a portion of the No-Man's Land and almost all the stable liquid phase ($200 < T < 370$ K). The data we obtain strongly support the hypothesis that these two temperatures play a central role in determining thermodynamic properties of both confined and bulk water, independent of the local environment. In the case of water confined on a protein, the experimental data strongly indicate that these two temperatures may define the biological functions of the protein.

ACKNOWLEDGMENTS

The research in Messina is supported by the IPCF-CNR. The research in Boston is supported by the National Science Foundation (NSF) Chemistry Division (Grant Nos. CHE 0911389, CHE 0908218, and CHE 1213217). C.C. thanks the Centro Studi di Fisica Nucleare e di Struttura della Materia (Catania, Italy).

[1] *Water Polymorphism*, Advances in Chemical Physics, edited by H. E. Stanley, series editor S. A. Rice (Wiley, New York, 2013).
[2] P. G. Debenedetti and H. E. Stanley, Phys. Today **56**, 40 (2003).
[3] O. Mishima, L. D. Calvert, and E. Whalley, Nature (London) **314**, 76 (1985).
[4] P. H. Poole, F. Sciortino, U. Essmann, and H. E. Stanley, Nature (London) **360**, 324 (1992).
[5] S. Sastry, P. G. Debenedetti, and F. Sciortino, Phys. Rev. E **53**, 6144 (1996).
[6] R. J. Speedy and C. A. Angell, J. Chem. Phys. **65**, 851 (1976).
[7] O. Mishima and H. E. Stanley, Nature (London) **396**, 329 (1998).
[8] C. A. Angell, Science **319**, 582 (2008).
[9] V. Holten, C. E. Bertand, M. A. Anisimov, and J. V. Sengers, J. Chem. Phys. **136**, 094507 (2012).
[10] E. B. Moore and V. Molinero, Nature (London) **479**, 506 (2011).
[11] F. Mallamace, Proc. Natl. Acad. Sci. U.S.A. **106**, 15097 (2009).
[12] P. Kumar, S. V. Buldyrev, S. R. Becker, P. H. Poole, F. W. Starr, and H. E. Stanley, Proc. Natl. Acad. Sci. U.S.A. **104**, 9575 (2007).
[13] E. B. Moore and V. Molinero, J. Chem. Phys. **132**, 244504 (2010).
[14] L. Liu, S.-H. Chen, A. Faraone, C. W. Yen, and C. Y. Mou, Phys. Rev. Lett. **95**, 117802 (2005).
[15] D. Banerjee, S. N. Bhat, S. V. Bhat, and D. Leporini, Proc. Natl. Acad. Sci. U.S.A. **106**, 11448 (2009).
[16] K. J. Tielrooij, N. Garcia-Araez, M. Bonn, and H. J. Bakker, Science **328**, 1006 (2010).
[17] D. A. Turton, J. Hunger, G. Hefter, R. Buchner, and K. Wynne, J. Chem. Phys. **128**, 161102 (2008).
[18] M. Karplus, Nat. Chem. Biol. **7**, 401 (2011).
[19] F. Parak and E. W. Knapp, Proc. Natl. Acad. Sci. U.S.A. **81**, 7088 (1984).
[20] I. E. T. Iben, D. Braunstein, W. Doster, H. Frauenfelder, M. K. Hong, J. B. Johnson, S. Luck, P. Ormos, A. Schulte, P. J. Steinbach, A. H. Xie, and R. D. Young, Phys. Rev. Lett. **62**, 1916 (1989).
[21] Y. Levy and J. N. Onuchic, Annu. Rev. Biophys. Biomol. Struct. **35**, 389 (2006).
[22] G. A. Jeffrey and W. Saenger, *Hydrogen Bonding in Biological Structures* (Springer-Verlag, Berlin, 1991).
[23] S.-H. Chen, F. Mallamace, C. Y. Mou, M. Broccio, C. Corsaro, A. Faraone, and L. Liu, Proc. Natl. Acad. Sci. U.S.A. **103**, 12974 (2006).
[24] F. Mallamace, M. Broccio, C. Corsaro, A. Faraone, D. Majolino, V. Venuti, L. Liu, C. Y. Mou, and S.-H. Chen, Proc. Natl. Acad. Sci. U.S.A. **104**, 424 (2007).
[25] W. Doster, H. Nakagawa, and M. S. Appavou, J. Chem. Phys. **139**, 045105 (2013); W. Doster, S. Busch, A. M. Gaspar, M. S. Appavou, J. Wuttke, and H. Scheer, Phys. Rev. Lett. **104**, 098101 (2010).
[26] G. Zaccai, Science **288**, 1604 (2000).
[27] V. Reat, R. Dunn, M. Ferrand, J. L. Finney, R. M. Daniel, and J. C. Smith, Proc. Natl. Acad. Sci. U.S.A. **97**, 9961 (2000).
[28] G. Schiro, F. Natali, and A. Cupane, Phys. Rev. Lett. **109**, 128102 (2012).
[29] K. L. Ngai, S. Capaccioli, and A. Pacciaroni, J. Chem. Phys. **138**, 235102 (2013).
[30] S. Pawlus, S. Khodadadi, and A. P. Sokolov, Phys. Rev. Lett. **100**, 108103 (2008).
[31] S.-H. Chen, L. Liu, E. Fratini, P. Baglioni, A. Faraone, and A. Mamontov, Proc. Natl. Acad. Sci. U.S.A. **103**, 9012 (2006).
[32] M. Vogel, Phys. Rev. Lett. **101**, 225701 (2008).
[33] H. Jansson and J. Swenson, Biochim. Biophys. Acta, Proteins Proteomics **1804**, 20 (2010); J. Swenson, H. Jansson, and R. Bergman, Phys. Rev. Lett. **96**, 247802 (2006).
[34] G. Caliskan, R. M. Briber, D. Thirumalai, V. Garcia-Sakai, S. A. Woodson, and A. P. Sokolov, J. Am. Chem. Soc. **128**, 32 (2006).
[35] F. Mallamace, C. Corsaro, D. Mallamace, P. Baglioni, H. E. Stanley, and S.-H. Chen, J. Phys. Chem. B **115**, 14280 (2011).
[36] M. Lagi, X. Chu, C. Kim, F. Mallamace, P. Baglioni, and S.-H. Chen, J. Phys. Chem. B **112**, 1571 (2008).
[37] Y. Zhang, M. Lagi, D. Liu, F. Mallamace, E. Fratini, P. Baglioni, E. Mamontov, M. Hagen, and S.-H. Chen, J. Chem. Phys. **130**, 135101 (2009).
[38] S.-H. Chen, L. Liu, X. Chu, Y. Zhang, E. Fratini, P. Baglioni, A. Faraone, and E. Mamontov, J. Chem. Phys. **125**, 171103 (2006).
[39] X. Q. Chu, E. Fratini, P. Baglioni, A. Faraone, and S.-H. Chen, Phys. Rev. E **77**, 011908 (2008).
[40] F. Mallamace, P. Baglioni, C. Corsaro, J. Spooren, H. E. Stanley, and S.-H. Chen, Riv. Nuovo Cimento **34**, 253 (2011).
[41] L. Xu, F. Mallamace, Z. Yan, F. W. Starr, S. V. Buldyrev, and H. E. Stanley, Nat. Phys. **5**, 565 (2009).
[42] K. Ito, C. T. Moynihan, and C. A. Angell, Nature (London) **398**, 492 (1999).
[43] F. Mallamace, C. Branca, C. Corsaro, N. Leone, J. Spooren, H. E. Stanley, and S.-H. Chen, J. Phys. Chem. B **114**, 1870 (2010).

[44]P. G. Debenedetti, *Metastable Liquids: Concepts and Principles* (Princeton University Press, Princeton, 1996).
[45]S. Yip and M. P. Short, Nat. Mater. **12**, 774 (2013).
[46]F. Mallamace, C. Corsaro, H. E. Stanley, and S.-H. Chen, Eur. Phys. J. E **34**, 94 (2011).
[47]F. Mallamace, C. Corsaro, and H. E. Stanley, Sci. Rep. **2**, 993 (2012).
[48]P. W. Bridgman, Proc. Am. Acad. Arts Sci. **47**, 441 (1912).
[49]G. S. Kell, J. Chem. Eng. Data **20**, 97 (1975).
[50]G. S. Kell and E. Whalley, J. Chem. Phys. **62**, 3496 (1975).
[51]C. M. Sorensen, J. Chem. Phys. **79**, 1455 (1983).
[52]D. E. Hare and C. M. Sorensen, J. Chem. Phys. **84**, 5085 (1986).
[53]D. E. Hare and C. M. Sorensen, J. Chem. Phys. **87**, 4840 (1987).
[54]O. Mishima, J. Chem. Phys. **133**, 144503 (2010).
[55]W. D. Wilson, J. Acoust. Soc. Am. **31**, 1067 (1959).
[56]K. Binder and W. Kob, *Glassy Materials and Disordered Solids* (World Scientific, River Edge, NJ, 2005).
[57]J. Jonas, Science **216**, 1179 (1982).
[58]V. Lubchenko and P. Wolynes, Annu. Rev. Phys. Chem. **58**, 235 (2007).
[59]G. Adam and J. Gibbs, J. Chem. Phys. **43**, 139 (1965).
[60]F. H. Stillinger, Science **267**, 1935 (1995).
[61]F. Mallamace, C. Corsaro, N. Leone, V. Villari, N. Micali, and S.-H. Chen, Sci. Rep. **4**, 3747 (2014).
[62]F. Mallamace, C. Branca, C. Corsaro, N. Leone, J. Spooren, S.-H. Chen, and H. E. Stanley, Proc. Natl. Acad. Sci. U.S.A. **107**, 22457 (2010).
[63]F. Mallamace, C. Corsaro, D. Mallamace, C. Vasi, and H. E. Stanley, Faraday Discuss. **167**, 95 (2013).
[64]J. C. Martinez-Garcia, J. Martinez-Garcia, S. J. Rzoska, and J. Hulliger, J. Chem. Phys. **137**, 064501 (2012).
[65]T. Hecksher, A. I. Nielsen, N. Boye Olsen, and J. C. Dyre, Nat. Phys. **4**, 737 (2008).
[66]J. C. Mauro, Y. Yue, A. J. Ellison, P. K. Gupta, and D. C. Allan, Proc. Natl. Acad. Sci. U.S.A. **106**, 19780 (2009).
[67]K. T. Wikfeldt, C. Huang, A. Nilsson, and L. G. M. Pettersson, J. Chem. Phys. **134**, 214506 (2011).
[68]K. T. Wikfeldt, A. Nilsson, and L. G. M. Pettersson, Phys. Chem. Chem. Phys. **13**, 19918 (2011).
[69]P. Taborek, R. N. Kleinman, and D. J. Bishop, Phys. Rev. B **34**, 1835 (1986).
[70]F. Mallamace, C. Corsaro, and H. E. Stanley, Proc. Natl. Acad. Sci. U.S.A. **110**, 4899 (2013).
[71]F. Mallamace, C. Corsaro, M. Broccio, C. Branca, N. Gonzalez-Segredo, J. Spooren, S.-H. Chen, and H. E. Stanley, Proc. Natl. Acad. Sci. U.S.A. **105**, 12725 (2008).
[72]E. O. Stejskal and J. E. Tanner, J. Chem. Phys. **42**, 288 (1965); W. S. Price, Concepts Magn. Reson. **10**, 197 (1998).
[73]M. Matubayasi, C. Wakai, and M. Nakahara, Phys. Rev. Lett. **78**, 2573 (1997).
[74]E. M. Purcell, H. C. Torrey, and R. V. Pound, Phys. Rev. **69**, 37 (1946).
[75]F. Bloch, Phys. Rev. **70**, 460 (1946).
[76]E. D. Becker, in *Encyclopedia of Nuclear Magnetic Resonance*, edited by D. M. Grant and R. K. Harris (Wiley, Chichester, 1996), p. 2409.
[77]D. Sebastiani and M. Parrinello, ChemPhysChem **3**, 675 (2002).
[78]D. G. Archer and R. W. Carter, J. Phys. Chem. B **104**, 8563 (2000).
[79]M. Oguni, Y. Kanke, and S. Namba, AIP Conf. Proc. **982**, 34 (2008).
[80]W. S. Price, I. Hiroyudi, and Y. Arata, J. Phys. Chem. A **103**, 448 (1999).
[81]J. H. Simpson and H. Y. Carr, Phys. Rev. **111**, 1201 (1958).
[82]E. W. Lang and L. Piculell, in *Water and Aqueous Solutions*, edited by G. W. Nelson and J. E. Enderby (Adam Hilger, Bristol, 1986), p. 31.
[83]W. T. Laughlin and D. R. Uhlmann, J. Phys. Chem. **76**, 2317 (1972).
[84]B. F. Rasmussen, A. M. Stock, D. Ringe, and G. A. Petsko, Nature (London) **357**, 423 (1992).
[85]J. A. Rupley and G. Careri, Adv. Protein Chem. **41**, 37 (1991).
[86]L. Pauling, R. B. Corey, and H. R. Branson, Proc. Natl. Acad. Sci. U.S.A. **37**, 205 (1951).
[87]M. Tarek and D. J. Tobias, Phys. Rev. Lett. **88**, 138101 (2002).
[88]F. Mallamace, C. Corsaro, P. Baglioni, E. Fratini, and S.-H. Chen, J. Phys.: Condens. Matter **24**, 064103 (2012).
[89]G. Salvetti, E. Tombari, L. Mikheeva, and G. P. Johari, J. Phys. Chem. B **106**, 6081 (2002).
[90]P. Kumar, Z. Yan, L. Xu, M. G. Mazza, S. V. Buldyrev, S. H. Chen, S. Sastry, and H. E. Stanley, Phys. Rev. Lett. **97**, 177802 (2006).
[91]P. G. de Gennes, *Scaling Concepts in Polymer Physics* (Cornell University Press, Ithaca, 1979).
[92]A. Cooper, Biophys. Chem. **115**, 89–97 (2005).
[93]M. Sundaralingam and Y. C. Serkharudu, Science **244**, 1333–1337 (1989).
[94]F. Mallamace, S. H. Chen, M. Broccio, C. Corsaro, V. Crupi, D. Majolino, V. Venuti, P. Baglioni, E. Fratini, C. Vannucci, and H. E. Stanley, J. Chem. Phys. **127**, 045104 (2007).